Title: Axon-terminals expressing EAAT2 (GLT-1; Slc1a2) are common in the forebrain and not limited to the hippocampus

Authors: Yun Zhou[1]; Bjørnar Hassel[2], Tore Eid[1, 3], Niels Christian Danbolt[1*]

Affiliations of all authors: 1. Neurotransporter Group, Department of Molecular Medicine, Institute of Basic Medical Sciences, University of Oslo, N-0317 Oslo, Norway; 2. Department of Complex Neurology and Neurohabilitation, Oslo University Hospital, University of Oslo, Oslo, Norway; 3. Department of Laboratory Medicine, Yale School of Medicine, New Haven, CT 06520, USA.

Running title: EAAT2 glutamate transporters in nerve endings

The exact number of words:

Abstract: 291

Introduction: 1140

To whom correspondence should be addressed: Niels Chr. Danbolt, Department of Anatomy, Institute of Basic Medical Sciences, University of Oslo, P.O.Box 1105 Blindern, N-0317 Oslo, NORWAY. Fax: (+47) 22 85 12 78, E-mail: n.c.danbolt@medisin.uio.no.

Keywords: Synaptosomes; Glutamate metabolism; Glutamate uptake; Excitatory amino acid transporter 2; Syn1-Cre; Presynaptic

ABBREVIATIONS

The abbreviations used are: CAS, Chemical Abstracts Service Registry Number; Cre, Cyclization recombinase; EAATs, excitatory amino acid transporters; EAAC1, excitatory amino acid carrier (EAAT3; slc1a1); EAATs, excitatory amino acid transporters; GLAST, glutamate aspartate transporter (EAAT1; slc1a3); EAAT2, glutamate transporter 2 (EAAT2; slc1a2); NaPi, sodium phosphate buffer with pH 7.4; SDS, sodium dodecyl sulfate; Syn1-EAAT2 knockout mice, mice resulting from crossing EAAT2-flox mice with synapsin 1-Cre mice; VGLUT, vesicular glutamate transporter; WT, wild-type mice.

Abstract

The excitatory amino acid transporter type 2 (EAAT2) represents the major mechanism for removal of extracellular glutamate. In the hippocampus, there is some EAAT2 in axon-terminals, whereas most of the protein is found in astroglia. The functional importance of the neuronal EAAT2 is unknown, and it is debated whether EAAT2 expressing nerve terminals are present in other parts of the brain. Here we selectively deleted the EAAT2 gene in neurons (by crossing EAAT2-flox mice with synapsin 1-Cre mice in the C57B6 background). To reduce interference from astroglial EAAT2, we measured glutamate accumulation in crude tissue homogenates. EAAT2 proteins levels were measured by immunoblotting. Although synapsin 1-Cre mediated gene deletion only reduced the forebrain tissue content of EAAT2 protein to 95.5 ± 3.4 % of wild-type (littermate) controls, the glutamate accumulation in homogenates of neocortex, hippocampus, striatum and thalamus were nevertheless diminished to, respectively, 54 ± 4, 46 ± 3, 46 ± 2 and 65 ± 7 % of controls (average ± SEM, n=3 pairs of littermates). GABA uptake was unaffected. After injection of U-^{13}C-glucose, lack of neuronal EAAT2 resulted in higher ^{13}C-labeling of glutamine and GABA in the hippocampus suggesting that neuronal EAAT2 is partly short-circuiting the glutamate-glutamine cycle in wild-type mice. Crossing synapsin 1-Cre mice with Ai9 reporter mice revealed that Cre-mediated excision occurred efficiently in hippocampus CA3, but less efficiently in other regions and hardly at all in the cerebellum. Conclusions: (1) EAAT2 is expressed in nerve terminals in multiple brain regions. (2) The uptake catalyzed by neuronal EAAT2 plays a role

in glutamate metabolism, at least in the hippocampus. (3) Synapsin 1-Cre does not delete floxed genes in all neurons, and the contribution of neuronal EAAT2 is therefore likely to be larger than revealed in the present study.

High-lights

- Nerve terminals expressing EAAT2 are widely distributed in the brain and are not limited to the hippocampus
- Deletion of neuronal EAAT2 leads re-routing of extracellular glutamate
- Synapsin 1-Cre mice does not delete floxed genes in all neurons. This raises the question if there are more EAAT2 in neurons than we managed to detect here.

1. **Introduction**

The importance of glutamate uptake for controlling the excitatory action of glutamate is well established (Danbolt, 2001; Tzingounis and Wadiche, 2007; Vandenberg and Ryan, 2013). There are five different glutamate (excitatory amino acid) transporters (EAATs) in the mammalian central nervous system. EAAT1 is selectively expressed in astroglial cells in the central nervous system (Lehre *et al.*, 1995), while EAAT3 (Holmseth *et al.*, 2012a) and EAAT4 (Dehnes *et al.*, 1998) are expressed in soma and dendrites of neurons. The most important subtype, however, is EAAT2 (GLT-1; slc1a2) which represents more than 95 % of the total glutamate uptake activity in the mature forebrain (Haugeto *et al.*, 1996; Otis and Kavanaugh, 2000). Mice lacking EAAT2 in the central nervous system have lethal spontaneous seizures starting at around three weeks of age (Tanaka *et al.*, 1997; Zhou *et al.*, 2014a) when wildtype animals already robustly express EAAT2 (Ullensvang *et al.*, 1997; Furuta *et al.*, 1997). The EAAT2 protein is known to be predominantly expressed in astroglia (Danbolt *et al.*, 1992; Levy *et al.*, 1993; Rothstein *et al.*, 1994; Lehre *et al.*, 1995), and selective deletion of the EAAT2 gene in astrocytes is sufficient to produce lethal spontaneous seizures (Petr *et al.*, 2015), while lack of the other EAAT-subtypes is not lethal (for review: Zhou and Danbolt, 2013).

Unresolved questions concern the presence and functional roles of EAAT2 in neurons (for review: Danbolt *et al.*, 2016a). Early electron microscopy data suggested that nerve terminals, at least in cortex and striatum, are able to take up glutamate (e.g. Beart, 1976; McLennan, 1976; Gundersen *et al.*, 1993),

though the responsible carrier(s) was not determined. Although EAAT2 mRNA is present in the majority of neurons in multiple CNS regions (Torp *et al.*, 1994; Schmitt *et al.*, 1996; Torp *et al.*, 1997; Berger and Hediger, 1998; Berger and Hediger, 2000; Berger and Hediger, 2001), initial studies failed to detect the EAAT2 protein in normal mature brain tissue (for review: Zhou and Danbolt, 2014) despite active searches for it. As EAAT2 protein was detected in retinal bipolar cells (Rauen, 2000; Harada *et al.*, 1998; Palmer *et al.*, 2003), in brain neurons during development (Northington *et al.*, 1998; Northington *et al.*, 1999), in neurons in diseased brain tissue (Martin *et al.*, 1997) and in cultured neurons (e.g. Mennerick *et al.*, 1998; Plachez *et al.*, 2000), it was assumed that several types of neurons have the potential to express EAAT2 although EAAT2 protein was not detected (for review, see section 4.2 in Danbolt, 2001).

The presence of glutamate transporters in axon-terminals has thereby been a puzzle (Zhou and Danbolt, 2014) until it was shown electron microscopically that terminals in CA1 (originating from the CA3 pyramidal cells) indeed express EAAT2 (Chen *et al.*, 2004; Furness *et al.*, 2008). Chen and co-workers (2004) used a pre-embedding peroxidase technique and counted labeled terminals. This revealed a substantial heterogeneity as only a subpopulation was labeled. Furness and co-workers (2008) used immunogold to permit quantification of the EAAT2 immunoreactivity and concluded that around 80 % of the gold particles were present over astrocytes, and that most of the remainder was associated with axons and terminals. As most of the labeled terminals were labeled with only one gold-particle, it was clear that the

immunogold method was stretched to its limits. About half of the terminals were unlabeled, but as 3/4 of the terminals were able to accumulate D-aspartate by an EAAT2-dependent mechanism, it was concluded that the majority of the terminals expressed EAAT2 and that EAAT2 is the only (significant) glutamate transporter in axon-terminals (Furness *et al.*, 2008).

The above studies focused on the hippocampus. Therefore it remains to be determined if EAAT2 is expressed in terminals elsewhere. Rather than using the immunogold method, which is labor intensive and has low sensitivity as explained above (see also: Zhou and Danbolt, 2014), a more cost-efficient method is needed if the whole brain is to be screened.

When examining tissue homogenates and synaptosomal preparations electron microscopically with respect to D-aspartate accumulation, it was noted that most of the uptake, even in crude hippocampal homogenates, occurred in the nerve terminals (Furness *et al.*, 2008). There was also labeling in some glial elements in agreement with others (Henn *et al.*, 1976; Nakamura *et al.*, 1993), but the predominance of nerve terminal labeling was remarkable considering the very high levels of EAAT2 in astrocytes and the low levels in terminals. Because of the high levels of internal glutamate it was hypothesized that this selectivity for neuronal EAAT2, rather than astroglial EAAT2, was due to differences in the relative rates of heteroexchange and net uptake, but that hypothesis was refuted (Zhou *et al.*, 2014b). Instead we hypothesized (Danbolt *et al.*, 2016a) that the selectivity was simply due to differences between pinched of terminals and glial fragments with respect to ability to form sealed compartments after

homogenization (Fig. 1). This was tested experimentally. Neuronal deletion of EAAT2 resulted in a large reduction in glutamate accumulation by synaptosomes and crude tissue homogenates despite minor reductions in total EAAT2 protein (Petr *et al.*, 2015) as predicted by electron microscopy (Furness *et al.*, 2008). In contrast, astroglial deletion of EAAT2 hardly affected the accumulation by synaptosomes (Petr *et al.*, 2015). However, when the same tissue homogenates were solubilized and the transporters reconstituted into artificial cell membranes, liposomes (Danbolt *et al.*, 1990; Trotti *et al.*, 1995), then the quantitative dominance of the astroglial EAAT2 was revealed (Petr *et al.*, 2015). This result was taken as support for the above notion that most of the astroglial EAAT2 in a crude homogenate resides in membranes that do not form tight comportments and thereby does not contribute to the measured uptake. But when all EAAT2 is taken out of the native membranes and inserted into new ones, then astroglial and neuronal EAAT2 molecules will both contribute, and as there are more astroglial EAAT2 molecules than neuronal ones, the astroglial ones dominate.

Here we combined this selective resealing (Furness *et al.*, 2008) with conditional deletion of the EAAT2 gene (Zhou *et al.*, 2014a) in order to screen for neuronal EAAT2. To include as many axon-terminal types as possible, we decided to use crude homogenates. We report that there is EAAT2 catalyzed glutamate uptake in terminals in various brain areas and thereby not only in the hippocampus. We also report that *i.p.* administration of ^{13}C-glucose leads to ^{13}C-labeling of several amino acids, including glutamate, glutamine and GABA. Loss of neuronal EAAT2 leads to an increase of ^{13}C-Labeling of glutamine and GABA

from ^{13}C glucose in hippocampus, suggesting increased reliance on uptake of extracellular glutamate into astroglia and GABAergic neurons in the absence of nerve terminal EAAT2. Finally, the synapsin 1-Cre line fails to express Cre in large subsets of neurons. This implies that the reported reductions in synaptosomal glutamate accumulation determined here probably represent underestimations of the contributions of neuronal EAAT2 mediated uptake.

2. Materials and Methods

2.1. Materials

N,N' methylene bisacrylamide was from Promega (Madison, WI, USA). Molecular mass markers for SDS polyacrylamide gel electrophoresis (SDS PAGE) and nitrocellulose sheets (0.22 µm pores, 100 % nitrocellulose) were from GE Healthcare (Buckinghamshire, UK). Paraformaldehyde was from Electron Microscopy Sciences (Hatfield, PA, USA), and glutaraldehyde was from TAAB (Reading, UK). L-[^{3}H]glutamic acid (52 Ci/mmol) and [^{3}H]GABA (89 Ci/mmol) were from Amersham (Buckinghamshire, UK). Sodium dodecyl sulfate (SDS) of high purity (>99 % C12 alkyl sulfate) and nitrocellulose filters (HAWP; 0.45 µm pores) were from Millipore (Carrigtwohill, C. Cork, Ireland). Electrophoresis equipment was from Hoefer Scientific Instruments (San Francisco, CA, USA). All other reagents were obtained from Sigma-Aldrich (St. Louis, MO, USA).

2.2. Animals

All animal studies were carried out in accordance with the European

Communities Council Directive of 24 November 1986 (86/609/EEC). Formal approval to conduct the experiments was obtained from the animal subjects review board of the Norwegian Governmental Institute of Public Health (Oslo, Norway). Care was taken to avoid suffering and minimize the number of the experimental animals. The mice were housed in individually ventilated (IVC) cages at constant temperature and humidity, and were fed with Harlan Teklad 2018 (Harlan Laboratories Inc., Indianapolis, IN, USA) with the assess to water *ad libitum* as described previously (Lehre *et al.*, 2011). Biopsies from ear or tail were collected for determining genotype (Zhou *et al.*, 2014a).

To be able to utilize the Cre-LoxP recombinase system (Gu *et al.*, 1993; Rajewsky *et al.*, 1996; Le and Sauer, 2000) we have previously tagged the EAAT2 gene (slc1a2) in mice by inserting a unique unidirectional DNA sequence (a "LoxP-site") before and after exon 3 and 4 in such a way that cyclization recombinase (Cre) mediated excision will result, not only in removal of the mentioned exons, but also in a frame shift preventing expression of a truncated protein. We hereafter refer to these mice as "EAAT2-flox mice" (MGI:5576462; B6.Cg-Slc1a2$^{tm1.1Ncd}$/J; RRID:IMSR_JAX:026619; Stock no. 026619; Jackson Laboratory; Zhou *et al.*, 2014a). [Genes with LoxP sites on each side are referred to as being "floxed" (an acronym for "flanking LoxP sites").]

Mice with Cre under control of the rat synapsin 1 promotor (B6.Cg-Tg(Syn1-cre)671Jxm/J; Rempe *et al.*, 2006; RRID:IMSR_JAX:003966; Stock no. 003966; Jackson Laboratory) are hereafter referred to as "synapsin 1-Cre mice". They express Cre selectively in neurons. Therefore, to selectively delete EAAT2

in neurons we crossed synapsin 1-Cre mice with EAAT2-flox mice. Experimental mice were produced from breeding homozygote EAAT2-flox mice (flox/flox) and mice heterozygote for both Cre and flox (flox/wt; Cre/0). This yielded control mice with normal EAAT2 expression ([flox/flox; 0/0] and [flox/wt; 0/0]) as well as homozygote knockout mice ([flox/flox; Cre/0]) from the same litters. These neuronal knockout mice are hereafter referred to as "Syn1-EAAT2 knockout". Both genders were used.

As the interpretation of the results depend on the specificity and efficiency of Cre-expression, it is imperative to validate the synapsin 1-Cre mice. To enable identification of cells lacking the floxed gene we crossed the synapsin 1-Cre mice (Cre/0) with homozygote Ai9 reporter mice (B6; 129S6-Gt(ROSA)$^{26Sortm9(CAG-tdTomato)Hze}$/J; Madisen *et al.*, 2010; RRID:IMSR_JAX:007905; Stock no. 007905; Jackson Laboratory). These mice harbor the gene encoding red fluorescent protein tdTomato, but in such a way that this protein is not expressed unless a floxed DNA stretch blocking expression is removed. Thus, when Cre is expressed in these mice, then expression of the red fluorescent protein tdTomato is permanently turned on in the cells themselves as well as in their descendants.

2.3. Antibodies

Affinity purified anti-peptide antibodies to sheep anti-EAAT2 (Ab#8; RRID:AB_2714090; Li *et al.*, 2012), rabbit anti-EAAT1 (GLAST; Ab#314; RRID:AB_2314561; Holmseth *et al.*, 2009) and rabbit anti-EAAT3 (EAAC1; Ab#371; RRID:AB_2714048; Holmseth *et al.*, 2012b) were from the same batch

as previously described. Because antibody batches may differ from each other (Danbolt *et al.*, 2016b), we identify antibody batches by the unique identification number ("Ab#") they are given by our electronic laboratory information system (software provided by Science Linker AS; Oslo, Norway).

Rabbit anti-VGLUT1 (Cat. No. 135303; RRID:AB_88787), rabbit anti-VGLUT2 (Cat. No. 135403; RRID:AB_1937236), mouse monoclonal anti-parvalbumin (Cl. 58E1; Cat. No. 195011G) and anti-Calbindin (D28K; Cat. No. 214011G) were gifts from Henrik Martens (Synaptic System GmbH, Goettingen, Germany). Mouse monoclonal anti-synaptophysin (Cat No. S5768; RRID:AB_477523) was purchased from Sigma (St. Louis, MO, USA). Mouse monoclonal anti-NeuN was obtained from Chemicon (Cat. No. MAB377; RRID:AB_2298772). IRDye 680RD Donkey anti-Rabbit IgG (H+L) (Cat. No. P/N 926-68073) and IRDye 800CW Donkey anti-mouse IgG (H+L) (Cat. No. P/N 926-32212) were from Li-Cor Bioscience UK Ltd and Alexa Fluor 680 AffiniPure Donkey anti-sheep IgG (H+L) (Cat. No. 713-625-147; RRID:AB_2340753) was from Jackson ImmunoResearch. Alexa fluor goat anti-mouse 488 antibodies were purchased from Molecular probes (Eugene, OR, USA).

2.4. L-[^{3}H]glutamate or [^{3}H]GABA uptake in crude synaptosomal preparations

Crude synaptosomal homogenates were prepared as described before (Thangnipon *et al.*, 1983). Mice (8-14 weeks old) were killed by cervical dislocation. The brains were rapidly removed, dissected and weighed. The dissected parts were immediately homogenized in 10 volumes ice-cold 0.32 M

sucrose using a motorized Potter-Elvehjem (glass-Teflon) homogenizer. The homogenates were diluted 1+ 9 in ice-cold 0.32 M sucrose and kept on ice until the use. Glutamate or GABA transport activities were determined as described previously (Levy *et al.*, 1995). Briefly, the uptake reactions (run in triplicate) were started by adding 50 µl of the above crude synaptosomes into 450 µl Krebs' solution with 1 µM radiolabeled amino acids (140 mM NaCl, 15 mM NaPi pH 7.4, 5 mM KCl, 10 mM Glucose, 1.2 mM $CaCl_2$, 1.2 mM $MgSO_4$ and 0.5 mg/ml BSA) at 30^{o}C. After incubation (1 min for glutamate uptake, 3 min for GABA uptake), the reactions were terminated by dilution in 2 ml ice-cold Krebs' solution and filtration through Millipore cellulose nitrate acetate filters (0.45 µm pores; Millipore, Darnstadt, Germany). The filters were washed and dissolved for liquid scintillation counting (Parckard Liquid Scintillation Analyzer 1900TR, PerkinElmer, Massachusetts, USA). One pair of knockout and control littermate mice was used in each experiment. The results are presented as percent of control (average ± SEM where n represents the number of independent experiments). Unpaired student's T-test was used to compare the means of two groups of data. P-values are given when there were statistically significant differences ($p < 0.05$) between the data from the Syn1-EAAT2 knockout mice and the control mice.

2.5. Tissue preparation for electrophoresis and immunoblotting

Tissue was homogenized in 10-20 volumes of 1% SDS in 10 mM sodium phosphate buffer with pH 7.4 (NaPi). The homogenates were then subjected to

SDS-polyacrylamide gel electrophoresis and immunoblotted as described (Holmseth *et al.*, 2009). Precise loading was ensured by first measuring the total protein concentrations of the homogenates by the method of Lowry (Lowry *et al.*, 1951). Then the samples were applied onto the gels using a Hamilton syringe (Hamilton Robotics, NV, USA). The protein actually transferred to the nitrocellulose membranes were checked using Ponceau-S stain in combination with REVERT total protein stain (Cat. no. P/N926-11010, Li-Cor Bioscience). Finally, identical blots were prepared in parallel and probed with different primary antibodies. Briefly, the blots were first rinsed in PBS (10 mM NaPi pH7.4 and 135 mM NaCl) and then were blocked (1 hour) with 0.05% (w/v) casein in PBS before incubating with primary antibodies in BSA (30mg/ml) in PBST (PBS with 1 ml/liter Tween 20 and 0.5 mg/ml NaN_3) overnight, room temperature. The membrane was rinsed (4x10 min) with PBST before incubation (1 hour) in secondary antibody solution (1:10000 - 1:20000). The membranes were subsequently rinsed several times with PBST and then PBS to remove residual Tween 20 before scanning using an infrared scanner (Licor Odyssey system, LI-COR Biotechnology-UK Ltd, Cambridge, UK). The scanner had two channels permitting double labeling and thereby offering more reliable comparisons. Densitometric data were extracted from the 16bit image files by means of the gel analyzer tool included in our electronic laboratory information system (software provided by Science Linker AS; Oslo, Norway). The results are presented as percent of control (average ± SEM where n represents the number of pairs of littermates) and are based on all three concentrations. The experiments have

been repeated independently with tissue from 3-4 pairs wild-type and knockout littermates. Unpaired student's T-test was used to compare the means of two groups of data. P-values are given when there were statistically significant differences ($p < 0.05$) between the data from the Syn1-EAAT2 knockout mice and the control mice. For in debt discussions about specificity controls and other methodological precautions, see our previous reports (e.g. Holmseth *et al.*, 2009; Holmseth *et al.*, 2012b; Danbolt *et al.*, 2016b).

2.6. Immunocytochemistry

Mice were perfusion-fixed as described previously (Danbolt *et al.*, 1998). Briefly, they were given a lethal dose of ZFR cocktail (at least 0.1 ml per 10 g body weight). ZRF is of a mixture of Zolazepam (3.3 mg/ml; CAS 31352-82-6), Tiletamine (3.3 mg/ml; CAS 14176-49-9), Xylazine (0.5 mg/ml; CAS 7361-61-7) and Fentanyl (2.6 µg/ml; CAS 437-38-7). After cessation of all reflexes, the mice were perfused first with 0.1 M NaPi pH7.4 to wash out blood and then immediately followed by 4 % formaldehyde in 0.1 M NaPi with or without 0.1 % glutaraldehyde, as stated, for five minutes. The relevant tissues were collected and immersed in fixative for about 2-3 hour at room temperature. Sections (40 µm thick) were cut from the fixed unfrozen tissue using a Vibratome 1000 plus® (Vibratome, Bannockburn, UK).

Immunofluorescent labeling was done as previously described (Holmseth *et al.*, 2009; Zhou *et al.*, 2012). Briefly, the sections were rinsed (3 x 5 min) in

TBST (TBS with 0.5 % Triton X-100), treated with 1 M ethanolamine in 0.1 M NaPi pH 7.4 for 30 min, washed in TBST, incubated (1 hour) in TBST containing 10 % newborn calf serum and 3 % bovine serum albumin followed by incubation with primary antibodies and finally with secondary antibodies (Alexa fluor goat anti-mouse 488, Molecular probes; Eugene, OR, USA) diluted 1:1000 dilution. After being washed 3 times with TBST, the sections were then mounted with ProLong Gold antiFade mountant with DAPI (ThermoFisher Cat. No. P36935) and examined using a Zeiss Axioplan 2 microscope equipped with a Zeiss LSM 510 meta confocal scanner head (Zeiss, Jena, Germany).

2.7. Tissue preparation for liquid chromatography – tandem mass spectrometry (LC/MS)

Wild type and KO mice that had been fasted overnight (with free access to water) received [U-^{13}C]glucose, 7.5 µmol/g bodyweight, as an intraperitoneal (i.p.) injection of a 0.5 mol/L solution. Fifteen minutes later, the animals were euthanized by cervical dislocation and both hippocampi were rapidly dissected from the brain, immersed into liquid N_2 and weighed in the frozen state. Nine parts (volume) of ice cold LC/MS grade methanol (Optima, Fisher Scientific, Waltham, MA) were added to one part (weight) of frozen brain tissue, followed by homogenization at maximum speed for 90 s in a bead beater using Lysing Matrix D as the bead material (FastPrep, MP Biomedicals, Solon, OH). The samples were centrifuged at 12,000 g at 4°C for 5 minutes and the supernatant was stored at -20°C until processing for LC/MS. Using the AccQ-Tag Ultra kit

(Waters, Milford, MA), 5 µL of undiluted and 5 µL of 1:10 diluted (in methanol) supernatant was derivatized according to the kit procedure using $U^{13}C$-valine as the internal standard. A set of five-level amino acid calibrators was prepared by dilutions of a stock amino acid solution made from freshly dissoved glutamine powder in water (Cat. # G3126, Sigma-Aldrich, St. Louis, MO) with commercial amino acid standard solutions added to it (Cat. # A6407 and A6282, Sigma-Aldrich). Quality control samples at three different concentrations were made by adding different lots of glutamine powder (Fluka, Sigma-Aldrich) and amino acid solution (Cat. # A9906, Sigma-Aldrich) to extensively dialyzed bovine serum. One set of calibrators and one set of quality controls were included in each batch of derivatized samples.

2.8. LC/MS

On the same day of derivatization, samples were run by LC/MS (Waters Acquity/Xevo TQD, Waters, Milford MA) as follows. Two µL of sample was injected onto a UPLC HSS T3 Column (100Å, 1.8 µm, 2.1 mm X 150 mm, Waters) kept at 40°C, followed by gradient elution using (A) 0.1% formic acid (LC/MS grade, Fisher Scientific) in LC/MS grade water (Optima, Fisher Scientific) and (B) 0.1% formic acid in acetonitrile (Optima, Fisher Scientific) at a flow rate of 0.5 mL/min. The eluent was sprayed into the source using atmospheric electrospray ionization in the positive mode. Using multiple reaction monitoring, the following ion transitions were detected. Glutamate, m+0 = 318.1>171.1, m+1 = 319.1>171.1, m+2 = 320.1>171.1, m+3 = 321.1>171.1, m+4 = 322.1>171.1

and m+5 = 323.1>171.1. Glutamine, m+0 = 317.1>171.1, m+1 = 318.1>171.1, m+2 = 319.1>171.1, m+3 = 320.1>171.1, m+4 = 321.1>171.1 and m+5 = 322.1>171.1. GABA, m+0 = 274.1>171.1, m+1 = 275.1>171.1, m+2 = 276.1>171.1, m+3 = 277.1>171.1, and m+4 = 278.1>171.1. Alanine, m+0 = 260.1>116.1, m+1 = 261.1>116.1, m+2 = 262.1>116.1, and m+3 = 263.1>116.1. Aspartate, m+0 = 304.1>171.1, m+1 = 305.1>171.1, m+2 = 306.1>171.1, m+3 = 307.1>171.1, and m+4 = 308.1>171.1. For U^{13}-C valine the following transition was used: 293.1>171.1. The area under the peak for each transition was calculated using MarkerLynx (Waters). For determination of isotope ratios, the area of the peak for the isotope of interest was divided by the area under the peak for all measured isotopes for the specific amino acid. For determination of absolute concentrations, the peak area of each amino acid was divided by the peak area of the internal standard. The ratios were compared with the ratios from the standard curve and expressed as µmol/L of eluent. The eluent values were next corrected for sample dilutions and tissue weights, and expressed as µmol/kg of brain tissue, using 1 kg/L as the density of brain tissue. Care was taken to choose peak areas and ratios that were within the linear range of the assay, and to use appropriately diluted samples if not within the range. We have used the above assay for concentration and isotope determinations for brain microdialysis samples, plasma samples and brain tissue samples in our laboratory for several years. The performance characteristics of the assay are as follows. Accuracy (>80%, determined by comparison with accurately weighed-in standards that were spiked in sample matrix), between-run precision for unlabeled and singly

labeled isotopes at natural abundance (coefficient of variation, CV <10% at the concentration levels encountered in this type of samples), for doubly-labeled isotopes at natural abundance (CV typically <20%). Lower limit of quantitation (LOQ), determined as the lowest sample concentration providing a between-run CV of 20%, was for unlabeled amino acids approximately 0.1 µmol/L. The assay was linear in the range of 0.1 to 50 µmol/L.

The percent ^{13}C enrichment of amino acids (alanine, glutamate, GABA, glutamine, aspartate) was calculated from the total amount of the amino acid in question and the m+3 (alanine) and the m+2 (glutamate, GABA, glutamine, aspartate) isotopomers. We chose to focus on these isotopomers, because the alanine m+3 represents uniformly labeled alanine, [U-^{13}C]alanine, which is formed from [U-^{13}C]pyruvate (pyruvate m+3), which is the glycolytic end product of [U-^{13}C]glucose. The glutamate m+2 (and its derivatives, GABA, glutamine, and aspartate) is formed when [U-^{13}C]pyruvate is metabolized by pyruvate dehydrogenase and enters the TCAC as [1,2-^{13}C]acetyl-CoA (acetyl-CoA m+2), leading to the formation of [4,5-^{13}C]glutamate and its derivatives [4,5-^{13}C]glutamine, [1,2-^{13}C]GABA, and [1,2-^{13}C]- and [3,4-^{13}C]aspartate, which are all detected as m+2 by LC/MS.

3. Results

3.1. Deletion of neuronal EAAT2 hardly affects integrity of glutamatergic synapses, but causes a significant reduction in synaptosomal L-[^{3}H]glutamate accumulation

Mice where EAAT2 had been selectively deleted in neurons (the Syn1-EAAT2 knockout mice) were unremarkable. They had normal body weight and appeared healthy (data not shown). This was expected based on earlier observations (Petr *et al.*, 2015) using another line of floxed EAAT2 in combination with the same synapsin 1-Cre line.

We then prepared synaptosome containing homogenates from entire forebrains from Syn1-EAAT2 knockout mice (8-14 weeks of age) and their Cre-negative littermates as controls. As shown (Fig. 2A) synaptosomes prepared from Syn1-EAAT2 knockout mice had lower glutamate uptake activities compared to the control mice (61 ± 5 %, n=3, $p<0.01$), but normal GABA uptake activity (96 ± 3 %; n=3). Both the glutamate and the GABA uptake activities in brain tissue from synapsin 1-Cre mice (8-14 weeks of age) were normal (Fig. 2C) implying that the reduction in glutamate uptake seen in the Syn1-EAAT2 knockout mice (Fig. 2A) was not an effect mediated by Cre alone.

To exclude the possibility that the reduction is not caused by a reduction in the number of glutamatergic synapses, immunoblots were prepared from forebrains as in Figure 1A and probed with antibodies to various marker proteins (Fig. 2B). The blots revealed that the total tissue content of EAAT2 was only reduced by a few percent (95 ± 3 %, n=3), and that the markers tested as controls were basically unaffected: EAAT1 (96 ± 2 %; n=4, $p<0.04$; glial marker; Lehre *et al.*, 1995), EAAT3 (98 ± 4 %, n=3; neuronal marker: Holmseth *et al.*, 2012a), synaptophysin (97 ± 10 %, n=3; presynaptic marker; Jahn *et al.*, 1985; Navone *et al.*, 1986), vesicular glutamate transporter 1 (VGLUT1) (90 ± 6 %,

n=3) and VGLUT2 (89 ± 9%, n=3; VGLUT1/2 are glutamatergic markers: Li *et al.*, 2013). Immunocytochemistry was performed on tissue from some other Syn1-EAAT2 knockout mice, but no differences were noted in agreement with the blots (Fig. 2D).

Thus, there was only a minor reduction in total forebrain EAAT2 protein in the Syn1-EAAT2 knockouts, but nevertheless a substantial reduction in L-[^{3}H]glutamate accumulationy as determined using crude synaptosome containing homogenates.

3.2. Deletion of neuronal EAAT2 reduces synaptosomal glutamate uptake in multiple brain regions and thereby not only in the hippocampus

Homogenates were subsequently prepared from various brain regions and assayed for glutamate and GABA uptake activities (Fig. 3). The uptake activities in the homogenates from the Syn1-EAAT2 knockouts are expressed as percent of those from the control mice (average ± SEM; p-values are given when less than 0.05): hippocampus (46 ± 3 %; n=3, $p<0.001$), striatum (46 ± 2 %, n=3, $p<0.001$), neocortex (54 ± 4 %, n=3, $p<0.004$), and thalamus (65 ± 7 %, n=3, $p<0.05$). Statistically significant differences between Syn1-EAAT2 knockout mice were neither found in the cerebellum (96 ± 4 %, n =4) nor in the brain stem (92 ± 3.5 %, n =3).

GABA uptake was measured in the same homogenates as part of the same experiments, and was found not to be affected to a statistically significant degree: hippocampus (100 ± 4.0 %, n =3), neocortex (96 ± 2 %, n=3), striatum

(109 ± 8 %, n=3), thalamus (104 ± 5 %, n=3), cerebellum (97 ± 4 %, n=4) and brain stem (108 ± 2 %, n=3).

3.3. Loss of neuronal EAAT2 leads to increased ^{13}C-labeling of glutamine and GABA from ^{13}C-glucose in hippocampus

Wildtype and Syn1-EAAT2 knockout mice had similar total levels of alanine, glutamate, glutamine, and GABA in the brain regions examined (hippocampus, neocortex, thalamus, and cerebellum), with no significant differences between the groups (data not shown).

In the hippocampus we found that the ^{13}C-labeling of alanine was significantly greater than that of glutamate in both wildtype and Syn1-EAAT2 knockout mice (Table 1; $p<0.005$; paired *t*-test), reflecting how the ^{13}C label in glucose first travels through glycolysis, labeling pyruvate as [U-^{13}C]pyruvate (which may be converted to alanine), before it enters the TCA cycle as [1,2-^{13}C]acetyl-CoA (acetyl-CoA m+2) and labels glutamate, glutamine, GABA, and aspartate with two ^{13}C carbons. The ^{13}C-labeling of alanine from [U-^{13}C]glucose was similar in the two groups, as was the labeling of glutamate. In contrast, ^{13}C-labeling of glutamine and GABA was significantly higher in the hippocampus from Syn1-EAAT2 knockout mice, being 15% and 10% higher, respectively (Table 1).

3.4. Cre expression in the synapsin 1-Cre mice do not occur in all neurons

As the results of the present study depend on the Cre-mediated recombination, we tested the efficiency of the synapsin 1-Cre construction by crossing these

mice with Ai9 reporter mice (Madisen *et al.*, 2010). Cells in the latter mice start expressing tdTomato once Cre has excised a piece of DNA blocking the expression. This particular reporter line was chosen because it is highly sensitive to low levels of Cre facilitating efficient identification of Cre-positive cell populations (Madisen *et al.*, 2010).

As expected from available data (Zhu *et al.*, 2001; Allan Brain Altas: http://mouse.brain-map.org), crossing of synapsin 1-Cre mice with the Ai9 reporter mice resulted in a widespread neuron selective expression of tdTomato in agreement with the notion that synapsin 1-Cre is active in multiple neuronal populations. However, we also noted that multiple neurons failed to turn on tdTomato expression. For instance, the cerebellar granule cells were tdTomato negative (Fig. 4). The few cerebellar neurons that were tdTomato positive were mostly a subpopulation of GABAergic neurons (Fig. 4). In the neocortex, Cre expression showed a laminar pattern with the highest frequency of tdTomato positive cells in layers IV and VI with intermediate frequency in layer V and the lowest frequency in layers II and III (Fig. 5). The pyramidal cells in hippocampus CA3 and the granule cells in the dentate gyrus were mostly positive, but many CA1 pyramidal cells and interneurons were negative (Fig. 6). There were also tdTomato negative neurons elsewhere, e.g. in the striatum where the vast majority were negative (Fig. 4D). The images shown here (Figs. 3-5) are from two month old mice, but two weeks old mice displayed a very similar pattern (data not shown) giving no indication that the result is age dependent.

4. DISCUSSION

4.1. Most brain EAAT2 protein remains after deletion in neurons

When tissue samples from another synapsin 1-Cre directed conditional EAAT2-knockout mouse line were immunoblotted to quantify the reduction in EAAT2 proteins, only a 2.4 % non-statistically significant reduction was found (Petr *et al.*, 2015). Here we repeated this, but using another EAAT2-flox line and an infrared Western blot scanner rather than photographic film in order to get more accurate measurements. In agreement with Petr and co-workers (2015), the reduction was so small that it was hard to obtain statistically significant data. The exact values we arrived at depended on what we used as loading control and on how we determined background, but appeared to be somewhere within the range 2-8 %. Thus, it was safe to conclude that the reduction in total tissue levels was minor. We did not pursue this to obtain more accurate values considering that the synapsin 1-Cre line was not active in all neurons (see below).

4.2. Neuronal EAAT2 expression is not limited to the hippocampus

Here we took advantage of the preference of the synaptosome assay for nerve terminally located transporters (Furness *et al.*, 2008; Petr *et al.*, 2015). This allowed us to quickly screen multiple brain regions for loss of neuronal EAAT2 activity following synapsin 1-Cre mediated deletion of floxed EAAT2. Deletion of the EAAT2 gene in neurons resulted in major reductions of glutamate uptake activities in homogenates from neocortex, striatum and thalamus in

addition to hippocampus suggesting that EAAT2 is expressed in terminals in all these regions.

4.3. Loss of neuronal EAAT2 leads to re-routing of extracellular glutamate

There were subtle, but statistically significant, changes in glutamate metabolism in Syn1-EAAT2 knockout mice, as evidenced by the increased ^{13}C-labeling of glutamine and GABA from [U-^{13}C]glucose (Fig. 7). ^{13}C-Labeling of glutamine from ^{13}C-glucose, reflects glial uptake of extracellular (neuronal) ^{13}C-glutamate to a high degree (Hassel *et al.*, 1997). The increased formation of ^{13}C-glutamine in the present study probably reflects increased proportion of extracellular ^{13}C-glutamate moving into astroglial cells with subsequent conversion to glutamine in the absence of neuronal glutamate uptake. Similarly, the increased formation of ^{13}C-GABA in Syn1-EAAT2 knockout mice could reflect increased dependence on uptake of extracellular ^{13}C-glutamate into GABAergic neurons through EAAT3 glutamate transporters, with subsequent conversion of ^{13}C-glutamate into GABA (Bjorn-Yoshimoto and Underhill, 2016).

4.4. Possible underestimation of neuronal EAAT2 expression

The strategy used in the present study to detect neuronal EAAT2 depends on the activity of the synapsin 1-Cre construction. Consequently, as the synapsin 1-Cre mice did not express Cre in the granule cells, our data are inconclusive with respect to the cerebellum.

Based on our own previous estimations of the distribution of nerve terminal uptake of D-aspartate (an EAAT substrate) in the hippocampus (Furness *et al.*, 2008), we concluded that about 85 % of the uptake occurred in terminals in the hippocampal synaptosome preparations. The 54 % reduction observed here (Fig. 3) may imply that some terminals still expressed EAAT2 considering that Cre was not expressed in all neurons.

In the neocortex we observed the most efficient Cre-expression in layers IV and VI with intermediate efficiency in layer V and low efficiency in layers II and III. The reported levels of neuronal EAAT2 mRNA in the various neocortical layers have been reported to be: II and III < IV and V < VI (Berger and Hediger, 1998). Although the deletion did not comprise all neurons, the highest efficiency has been where most of the neuronal EAAT2 mRNA is. Nevertheless, it seems plausible that the glutamate accumulation in neocortical synaptosomes would have been even lower than the 46 % reduction observed here if the deletion had taken place in all neurons.

Only a small proportion of striatal neurons were Cre-positive. However, striatum receives afferent fibers from the neocortex and from thalamus. Most of the corticostriatal fibers come from layer V, but some come from layers III and VI (Paxinos, 2004). Thus, the reductions in glutamate accumulation in striatal synaptosomes are probably due to loss of EAAT2 in these axon-terminals. This interpretation is compatible with electron microscopy data showing D-aspartate uptake into striatal terminals (Gundersen *et al.*, 1996). Further, lesioning of the corticostriatal pathway reduces the synaptosomal glutamate accumulation in the

striatum to about 45 % (Fonnum *et al.*, 1981; Levy *et al.*, 1995). This value is similar to the value reported here, but in the former studies only cortical neurons were ablated, while the present study involved both (but incompletely) neocortex and thalamus. Unfortunately, our data are inconclusive with respect to the cerebellum as the synapsin 1-Cre mice did not express Cre in the granule cells.

No attempts were made to detect remaining EAAT2 by means of immunocytochemistry because EAAT2 is hard to detect in axon-terminals. This is after all the reason why it went undetected for about 10 years despite being searched for.

4.5. A widespread occurrence of EAAT2 in nerve terminals reconciles conflicting data

The data presented here suggest that EAAT2 protein is expressed, and is functional, in multiple classes of nerve terminals. This implies a widespread expression of EAAT2 in neurons although the expression levels are lower than those in astrocytes. This conclusion has been controversial, but it agrees well with a large number of reports. For instance, EAAT2 eGFP BAC reporter mice display high levels of EAAT2 promotor activity in most astrocytes, but also in several neuronal populations (including 80 % of the CA3 pyramidal cells), albeit at considerably lower levels than in astrocytes (De Vivo *et al.*, 2010). *In-situ* hybridization studies also concluded that EAAT2 mRNA is present in several neuronal populations (see the Introduction for references). Finally, several recent

studies report EAAT2 immunoreactivity in additional types of terminals (e.g. Arranz *et al.*, 2008; Melone *et al.*, 2009; Melone *et al.*, 2011).

Although EAAT2 may be expressed in more terminals than is currently recognized, it should be kept in mind that some terminals do not express functional transporters. A clear example is the Calyx of Held synapse in the brainstem, which is large enough to permit patch-clamp recordings and thereby direct investigation (see: von Gersdorff and Borst, 2002; Billups *et al.*, 2013).

4.6. Conclusions

(1) We reproduce results obtained with another EAAT2-flox line (Slc1A2tm1.1Pros; MGI: 5752263: Petr *et al.*, 2015). Deletion of neuronal EAAT2 has minor impact on total EAAT2 levels and is thereby unlikely to impact the total glutamate uptake activity in the living brain. (2) Deletion of EAAT2 in neurons results in substantial reductions in glutamate uptake measured in synaptosome containing tissue homogenates from various brain regions. This strongly suggests that EAAT2 is functionally expressed in multiple types of nerve terminals and thereby not only in those projecting from hippocampal CA3 pyramidal cells to CA1. (3) Higher ^{13}C-labelings of glutamine and GABA were found in Syn1-EAAT2 knockout mice, suggesting increased uptake of extracellular ^{13}C-labeled glutamate into astroglia and GABAergic neurons, respectively. (4) The synapsin 1-Cre line does not express Cre in all neurons. While most hippocampal CA3 pyramidal neurons were Cre-positive, most of the cerebellar granule cells were negative. This raises the question if there are more

EAAT2 in neurons than we managed to detect here. (5) The data reported earlier (Petr *et al.*, 2015) and those presented here may thereby represent underestimations of the contributions and tissue content of EAAT2 protein because of the limitations of the synapsin 1-Cre line.

Acknowledgements

This work was supported by the Norwegian Research Council (grant 240844), Novo Nordisk Fonden (grant NNF14OC0010959; NNF150C0016528), and by the University of Oslo (SERTA and UNIFOR).

References

Arranz, A.M., Hussein, A., Alix, J.J., Perez-Cerda, F., Allcock, N., Matute, C., Fern, R., 2008. Functional glutamate transport in rodent optic nerve axons and glia. Glia 56, (12) 1353-1367.

Beart, P.M., 1976. The autoradiographic localization of L-(3H) glutamate in synaptosomal preparations. Brain Res 103, (2) 350-355.

Berger, U.V., Hediger, M.A., 1998. Comparative analysis of glutamate transporter expression in rat brain using differential double in situ hybridization. Anat Embryol (Berl) 198, (1) 13-30.

Berger, U.V., Hediger, M.A., 2000. Distribution of the glutamate transporters GLAST and GLT-1 in rat circumventricular organs, meninges, and dorsal root ganglia. J Comp Neurol 421, (3) 385-399.

Berger, U.V., Hediger, M.A., 2001. Differential distribution of the glutamate transporters GLT-1 and GLAST in tanycytes of the third ventricle. J Comp Neurol 433, (1) 101-114.

Billups, D., Marx, M.-C., Mela, I., Billups, B., 2013. Inducible presynaptic glutamine transport supports glutamatergic transmission at the calyx of Held synapse. J Neurosci 33, (44) 17429-17434.

Bjorn-Yoshimoto, W.E., Underhill, S.M., 2016. The importance of the excitatory amino acid transporter 3 (EAAT3). Neurochem Int 98, () 4-18.

Chen, W., Mahadomrongkul, V., Berger, U.V., Bassan, M., DeSilva, T., Tanaka, K., Irwin, N., Aoki, C., Rosenberg, P.A., 2004. The glutamate transporter GLT1a is expressed in excitatory axon terminals of mature hippocampal neurons. J Neurosci 24, (5) 1136-1148.

Danbolt, N.C., 2001. Glutamate uptake. Prog Neurobiol 65, (1) 1-105.

Danbolt, N.C., Furness, D.N., Zhou, Y., 2016a. Neuronal vs glial glutamate uptake: Resolving the conundrum. Neurochem Int 98, () 29-45.

Danbolt, N.C., Lehre, K.P., Dehnes, Y., Chaudhry, F.A., Levy, L.M., 1998. Localization of transporters using transporter-specific antibodies. Methods Enzymol 296, () 388-407.

Danbolt, N.C., Pines, G., Kanner, B.I., 1990. Purification and reconstitution of the sodium- and potassium-coupled glutamate transport glycoprotein from rat brain. Biochemistry 29, (28) 6734-6740.

Danbolt, N.C., Storm-Mathisen, J., Kanner, B.I., 1992. An [Na+ + K+]coupled L-glutamate transporter purified from rat brain is located in glial cell processes. Neuroscience 51, (2) 295-310.

Danbolt, N.C., Zhou, Y., Furness, D.N., Holmseth, S., 2016b. Strategies for immunohistochemical protein localization using antibodies: What did we learn from neurotransmitter transporters in glial cells and neurons. Glia 64, (12) 2045-2064.

De Vivo, L., Melone, M., Rothstein, J.D., Conti, F., 2010. GLT-1 Promoter Activity in Astrocytes and Neurons of Mouse Hippocampus and Somatic Sensory Cortex. Front Neuroanat 3, () 31.

Dehnes, Y., Chaudhry, F.A., Ullensvang, K., Lehre, K.P., Storm-Mathisen, J., Danbolt, N.C., 1998. The glutamate transporter EAAT4 in rat cerebellar Purkinje cells: a glutamate-gated chloride channel concentrated near the synapse in parts of the dendritic membrane facing astroglia. J Neurosci 18, (10) 3606-3619.

Fonnum, F., Storm-Mathisen, J., Divac, I., 1981. Biochemical evidence for glutamate as neurotransmitter in corticostriatal and corticothalamic fibres in rat brain. Neuroscience 6, (5) 863-873.

Furness, D.N., Dehnes, Y., Akhtar, A.Q., Rossi, D.J., Hamann, M., Grutle, N.J., Gundersen, V., Holmseth, S., Lehre, K.P., Ullensvang, K., Wojewodzic, M., Zhou, Y., Attwell, D., Danbolt, N.C., 2008. A quantitative assessment of glutamate uptake into hippocampal synaptic terminals and astrocytes: new insights into a neuronal role for excitatory amino acid transporter 2 (EAAT2). Neuroscience 157, (1) 80-94.

Furuta, A., Rothstein, J.D., Martin, L.J., 1997. Glutamate transporter protein subtypes are expressed differentially during rat CNS development. J Neurosci 17, (21) 8363-8375.

Gu, H., Zou, Y.R., Rajewsky, K., 1993. Independent control of immunoglobulin switch recombination at individual switch regions evidenced through Cre-loxP-

mediated gene targeting. Cell 73, (6) 1155-1164.

Gundersen, V., Danbolt, N.C., Ottersen, O.P., Storm-Mathisen, J., 1993. Demonstration of glutamate/aspartate uptake activity in nerve endings by use of antibodies recognizing exogenous D-aspartate. Neuroscience 57, (1) 97-111.

Gundersen, V., Ottersen, O.P., Storm-Mathisen, J., 1996. Selective excitatory amino acid uptake in glutamatergic nerve terminals and in glia in the rat striatum: quantitative electron microscopic immunocytochemistry of exogenous (D)-aspartate and endogenous glutamate and GABA. Eur J Neurosci 8, (4) 758-765.

Harada, T., Harada, C., Watanabe, M., Inoue, Y., Sakagawa, T., Nakayama, N., Sasaki, S., Okuyama, S., Watase, K., Wada, K., Tanaka, K., 1998. Functions of the two glutamate transporters GLAST and GLT-1 in the retina. Proc Natl Acad Sci U S A 95, (8) 4663-4666.

Hassel, B., Bachelard, H., Jones, P., Fonnum, F., Sonnewald, U., 1997. Trafficking of amino acids between neurons and glia in vivo. Effects of inhibition of glial metabolism by fluoroacetate. J Cereb Blood Flow Metab 17, (11) 1230-1238.

Haugeto, Ø., Ullensvang, K., Levy, L.M., Chaudhry, F.A., Honore, T., Nielsen, M., Lehre, K.P., Danbolt, N.C., 1996. Brain glutamate transporter proteins form

homomultimers. J Biol Chem 271, (44) 27715-27722.

Henn, F.A., Anderson, D.J., Rustad, D.G., 1976. Glial contamination of synaptosomal fractions. Brain Res 101, () 341-344.

Holmseth, S., Dehnes, Y., Huang, Y.H., Follin-Arbelet, V.V., Grutle, N.J., Mylonakou, M.N., Plachez, C., Zhou, Y., Furness, D.N., Bergles, D.E., Lehre, K.P., Danbolt, N.C., 2012a. The density of EAAC1 (EAAT3) glutamate transporters expressed by neurons in the mammalian CNS. J Neurosci 32, (17) 6000-6013.

Holmseth, S., Scott, H.A., Real, K., Lehre, K.P., Leergaard, T.B., Bjaalie, J.G., Danbolt, N.C., 2009. The concentrations and distributions of three C-terminal variants of the GLT1 (EAAT2; slc1a2) glutamate transporter protein in rat brain tissue suggest differential regulation. Neuroscience 162, (4) 1055-1071.

Holmseth, S., Zhou, Y., Follin-Arbelet, V.V., Lehre, K.P., Bergles, D.E., Danbolt, N.C., 2012b. Specificity controls for immunocytochemistry: the antigen pre-adsorption test can lead to inaccurate assessment of antibody specificity. J Histochem Cytochem 60, (3) 174-187.

Jahn, R., Schiebler, W., Ouimet, C., Greengard, P., 1985. A 38,000-dalton membrane protein (p38) present in synaptic vesicles. Proc Natl Acad Sci U S A

82, (12) 4137-4141.

Le, Y., Sauer, B., 2000. Conditional gene knockout using cre recombinase. Methods Mol Biol 136, () 477-485.

Lehre, A.C., Rowley, N.M., Zhou, Y., Holmseth, S., Guo, C., Holen, T., Hua, R., Laake, P., Olofsson, A.M., Poblete-Naredo, I., Rusakov, D.A., Madsen, K.K., Clausen, R.P., Schousboe, A., White, H.S., Danbolt, N.C., 2011. Deletion of the betaine-GABA transporter (BGT1; slc6a12) gene does not affect seizure thresholds of adult mice. Epilepsy Res 95, (1-2) 70-81.

Lehre, K.P., Levy, L.M., Ottersen, O.P., Storm-Mathisen, J., Danbolt, N.C., 1995. Differential expression of two glial glutamate transporters in the rat brain: quantitative and immunocytochemical observations. J Neurosci 15, (3 Pt 1) 1835-1853.

Levy, L.M., Lehre, K.P., Rolstad, B., Danbolt, N.C., 1993. A monoclonal antibody raised against an [Na(+)+K+]coupled L-glutamate transporter purified from rat brain confirms glial cell localization. FEBS Lett 317, (1-2) 79-84.

Levy, L.M., Lehre, K.P., Walaas, S.I., Storm-Mathisen, J., Danbolt, N.C., 1995. Down-regulation of glial glutamate transporters after glutamatergic denervation in the rat brain. Eur J Neurosci 7, (10) 2036-2041.

Li, D., Herault, K., Silm, K., Evrard, A., Wojcik, S., Oheim, M., Herzog, E., Ropert, N., 2013. Lack of evidence for vesicular glutamate transporter expression in mouse astrocytes. J Neurosci 33, (10) 4434-4455.

Li, Y., Zhou, Y., Danbolt, N.C., 2012. The rates of postmortem proteolysis of glutamate transporters differ dramatically between cells and between transporter subtypes. J Histochem Cytochem 60, (11) 811-821.

Lowry, O.H., Rosebrough, N.J., Farr, A.L., Randall, R.J., 1951. Protein measurement with the Folin phenol reagent. J Biol Chem 193, (1) 265-275.

Madisen, L., Zwingman, T.A., Sunkin, S.M., Oh, S.W., Zariwala, H.A., Gu, H., Ng, L.L., Palmiter, R.D., Hawrylycz, M.J., Jones, A.R., Lein, E.S., Zeng, H., 2010. A robust and high-throughput Cre reporting and characterization system for the whole mouse brain. Nat Neurosci 13, (1) 133-140.

Martin, L.J., Brambrink, A.M., Lehmann, C., Portera-Cailliau, C., Koehler, R., Rothstein, J., Traystman, R.J., 1997. Hypoxia-ischemia causes abnormalities in glutamate transporters and death of astroglia and neurons in newborn striatum. Ann Neurol 42, (3) 335-348.

McLennan, H., 1976. The autoradiographic localization of L-[3h]glutamate in rat

brain tissue. Brain Res 115, (1) 139-144.

Melone, M., Bellesi, M., Conti, F., 2009. Synaptic localization of GLT-1a in the rat somatic sensory cortex. Glia 57, (1) 108-117.

Melone, M., Bellesi, M., Ducati, A., Iacoangeli, M., Conti, F., 2011. Cellular and Synaptic Localization of EAAT2a in Human Cerebral Cortex. Front Neuroanat 4, () 151.

Mennerick, S., Dhond, R.P., Benz, A., Xu, W., Rothstein, J.D., Danbolt, N.C., Isenberg, K.E., Zorumski, C.F., 1998. Neuronal expression of the glutamate transporter GLT-1 in hippocampal microcultures. J Neurosci 18, (12) 4490-4499.

Nakamura, Y., Iga, K., Shibata, T., Shudo, M., Kataoka, K., 1993. Glial plasmalemmal vesicles: a subcellular fraction from rat hippocampal homogenate distinct from synaptosomes. Glia 9, (1) 48-56.

Navone, F., Jahn, R., Di Gioia, G., Stukenbrok, H., Greengard, P., De Camilli, P., 1986. Protein p38: an integral membrane protein specific for small vesicles of neurons and neuroendocrine cells. J Cell Biol 103, (6 Pt 1) 2511-2527.

Northington, F.J., Traystman, R.J., Koehler, R.C., Martin, L.J., 1999. GLT1, glial glutamate transporter, is transiently expressed in neurons and develops

astrocyte specificity only after midgestation in the ovine fetal brain. J Neurobiol 39, (4) 515-526.

Northington, F.J., Traystman, R.J., Koehler, R.C., Rothstein, J.D., Martin, L.J., 1998. Regional and cellular expression of glial (GLT1) and neuronal (EAAC1) glutamate transporter proteins in ovine fetal brain. Neuroscience 85, (4) 1183-1194.

Otis, T.S., Kavanaugh, M.P., 2000. Isolation of current components and partial reaction cycles in the glial glutamate transporter EAAT2. J Neurosci 20, (8) 2749-2757.

Palmer, M.J., Taschenberger, H., Hull, C., Tremere, L., von Gersdorff, H., 2003. Synaptic activation of presynaptic glutamate transporter currents in nerve terminals. J Neurosci 23, (12) 4831-4841.

Paxinos G, 2004. The rat nervous system. Elsevier Academic Press,. Amsterdam ;Boston :. ppxvii, 1309 p. : ill. (some col.) ; 29 cm..

Petr, G.T., Sun, Y., Frederick, N.M., Zhou, Y., Dhamne, S.C., Hameed, M.Q., Miranda, C., Bedoya, E.A., Fischer, K.D., Armsen, W., Wang, J., Danbolt, N.C., Rotenberg, A., Aoki, C.J., Rosenberg, P.A., 2015. Conditional deletion of the glutamate transporter GLT-1 reveals that astrocytic GLT-1 protects against fatal

epilepsy while neuronal GLT-1 contributes significantly to glutamate uptake into synaptosomes. J Neurosci 35, (13) 5187-5201.

Plachez, C., Danbolt, N.C., Recasens, M., 2000. Transient expression of the glial glutamate transporters GLAST and GLT in hippocampal neurons in primary culture. J Neurosci Res 59, (5) 587-593.

Rajewsky, K., Gu, H., Kuhn, R., Betz, U.A., Muller, W., Roes, J., Schwenk, F., 1996. Conditional gene targeting. J Clin Invest 98, (3) 600-603.

Rauen, T., 2000. Diversity of glutamate transporter expression and function in the mammalian retina. Amino Acids 19, (1) 53-62.

Rempe, D., Vangeison, G., Hamilton, J., Li, Y., Jepson, M., Federoff, H.J., 2006. Synapsin I Cre transgene expression in male mice produces germline recombination in progeny. Genesis 44, (1) 44-49.

Rothstein, J.D., Martin, L., Levey, A.I., Dykes-Hoberg, M., Jin, L., Wu, D., Nash, N., Kuncl, R.W., 1994. Localization of neuronal and glial glutamate transporters. Neuron 13, (3) 713-725.

Schmitt, A., Asan, E., Puschel, B., Jons, T., Kugler, P., 1996. Expression of the glutamate transporter GLT1 in neural cells of the rat central nervous system:

non-radioactive in situ hybridization and comparative immunocytochemistry. Neuroscience 71, (4) 989-1004.

Tanaka, K., Watase, K., Manabe, T., Yamada, K., Watanabe, M., Takahashi, K., Iwama, H., Nishikawa, T., Ichihara, N., Kikuchi, T., Okuyama, S., Kawashima, N., Hori, S., Takimoto, M., Wada, K., 1997. Epilepsy and exacerbation of brain injury in mice lacking the glutamate transporter GLT-1. Science 276, (5319) 1699-1702.

Thangnipon, W., Taxt, T., Brodal, P., Storm-Mathisen, J., 1983. The corticopontine projection: axotomy-induced loss of high affinity L-glutamate and D-aspartate uptake, but not of gamma-aminobutyrate uptake, glutamate decarboxylase or choline acetyltransferase, in the pontine nuclei. Neuroscience 8, (3) 449-457.

Torp, R., Danbolt, N.C., Babaie, E., Bjørås, M., Seeberg, E., Storm-Mathisen, J., Ottersen, O.P., 1994. Differential expression of two glial glutamate transporters in the rat brain: an in situ hybridization study. Eur J Neurosci 6, (6) 936-942.

Torp, R., Hoover, F., Danbolt, N.C., Storm-Mathisen, J., Ottersen, O.P., 1997. Differential distribution of the glutamate transporters GLT1 and rEAAC1 in rat cerebral cortex and thalamus: an in situ hybridization analysis. Anat Embryol (Berl) 195, (4) 317-326.

Trotti, D., Volterra, A., Lehre, K.P., Rossi, D., Gjesdal, O., Racagni, G., Danbolt, N.C., 1995. Arachidonic acid inhibits a purified and reconstituted glutamate transporter directly from the water phase and not via the phospholipid membrane. J Biol Chem 270, (17) 9890-9895.

Tzingounis, A.V., Wadiche, J.I., 2007. Glutamate transporters: confining runaway excitation by shaping synaptic transmission. Nat Rev Neurosci 8, (12) 935-947.

Ullensvang, K., Lehre, K.P., Storm-Mathisen, J., Danbolt, N.C., 1997. Differential developmental expression of the two rat brain glutamate transporter proteins GLAST and GLT. Eur J Neurosci 9, (8) 1646-1655.

Vandenberg, R.J., Ryan, R.M., 2013. Mechanisms of glutamate transport. Physiol Rev 93, (4) 1621-1657.

von Gersdorff, H., Borst, J.G., 2002. Short-term plasticity at the calyx of Held. Nat Rev Neurosci 3, (1) 53-64.

Zhou, Y., Danbolt, N.C., 2014. Glutamate as a neurotransmitter in the healthy brain. J Neural Transm 121, (8) 799-817.

Zhou, Y., Danbolt, N.C., 2013. GABA and Glutamate Transporters in Brain. Front Endocrinol (Lausanne) 4, () 165.

Zhou, Y., Holmseth, S., Hua, R., Lehre, A.C., Olofsson, A.M., Poblete-Naredo, I., Kempson, S.A., Danbolt, N.C., 2012. The betaine-GABA transporter (BGT1, slc6a12) is predominantly expressed in the liver and at lower levels in the kidneys and at the brain surface. Am J Physiol Renal Physiol 302, (3) F316-328.

Zhou, Y., Waanders, L.F., Holmseth, S., Guo, C., Berger, U.V., Li, Y., Lehre, A.-C., Lehre, K.P., Danbolt, N.C., 2014a. Proteome analysis and conditional deletion of the EAAT2 glutamate transporter provide evidence against a role of EAAT2 in pancreatic insulin secretion in mice. J Biol Chem 289, (3) 1329-1344.

Zhou, Y., Wang, X., Tzingounis, A.V., Danbolt, N.C., Larsson, H.P., 2014b. EAAT2 (GLT-1; slc1a2) glutamate transporters reconstituted in liposomes argues against heteroexchange being substantially faster than net uptake. J Neurosci 34, (40) 13472-13485.

Zhu, Y., Romero, M.I., Ghosh, P., Ye, Z., Charnay, P., Rushing, E.J., Marth, J.D., Parada, L.F., 2001. Ablation of NF1 function in neurons induces abnormal development of cerebral cortex and reactive gliosis in the brain. Genes Dev 15, (7) 859-876.

Figure legends

Figure 1. Schematic illustration of astroglial and axon-terminal fragments in a crude homogenate from wild-type (A) and Syn1-EAAT2 knockout mice (B). The astroglial membranes (**black lines**) have the highest density of EAAT2 molecules (**black dots**), but most of the membrane fragments fail to reseal. Thus glutamate (red asterisks) will only accumulate in a minority of them. In contrast, nerve terminal membranes (**blue lines**) have a higher probability of resealing leaving a higher proportion of them with active uptake. Thus, despite lower numbers of EAAT2 molecules, they are relatively dominant in the synaptosome assay explaining why deletion of the few percent of the EAAT2 expressed in neurons leads to a significant loss of glutamate accumulation in the synaptosomes.

Figure 2. Deletion of EAAT2 in neurons leads to reduced glutamate uptake activity in crude forebrain synaptosomes without reducing GABA uptake (A; n=3). Despite substantial reduction oin transport activity, there is only mild reduction in total EAAT2 protein as determined by immunoblotting (B; Ab#8; 0.3 µg/ml). Also note that there is little or no reduction in EAAT1 (Ab#314; 0.1 µg/ml) or EAAT3 (Ab#371; 1 µg/ml). Further, there is no change in markers for nerve terminals (synaptophysin, 1: 1000; VGLUT1, 0.3 µg/ml and VGLUT2, 0.3 µg/ml). The reduced uptake activity was not due to the presence of Cre, as synaptosomes prepared from Cre mice can take equal amount of 3H-glutamate and 3H-GABA

as that of its wildtype littermates (C; n =3). Immunoperoxidase labeling shows the dominant presence of astroglial EAAT2 in neuronal EAAT2 cKOs (D). scale bar 500 µm.

Figure 3. Crude synaptosome containing homogenates were prepared from different brain regions of Syn1-EAAT2 knockout mice (nKO) and their littermates (WT). Note that there are strong reductions in glutamate uptake activity (and not in GABA uptake activity) in several brain regions.

Figure 4. Low proportion of Cre-expressing cells in the cerebellum (Panels A-C) and striatum (Panel D) of synapsin 1-Cre mice crossed with Ai9 reporter mice. Cells in the Ai9 reporter mice start expressing red fluorescent tdTomato when Cre-mediated excision has taken place. Thus, if Cre has been sufficiently expressed at one point in time, the cells will stay red. Antibodies to neuronal markers NeuN (green; 1: 500; Panels A and D) and parvalbumin (Parv, green; 1 µg/ml; Panels B and C) were used to visualize neurons. Panel A: Very few, if any, granular cells (gr) were Cre-positive. Panels B and C: Also some of the parvalbumin positive (GABAergic) cells were Cre-negative. Arrowhead indicates a Cre-negative Purkinje cell. Panel D: The majority of the neurons in the striatum were Cre-negative. One of the few positive neurons is indicated (arrowhead). Blue DAPI labelled astrocyte nuclei are hard to see in these images. Scale bars: 50 µm in A and 20 µm in B-D.

Figure 5. Laminar Cre-expression in the neocortex of synapsin 1-Cre mice crossed with Ai9 reporter mice (see figure 3). Antibodies to neuronal markers NeuN (green; 1: 500; Panels A and B) and calbindin (Calb, green; 1 µg/ml; Panels C and D) were used to visualize neurons. Panels A-C: Note that large numbers of cortical neurons did not express Cre. Cre was mostly expressed in neurons in layers I, IV and VI. The lowest proportion of Cre-positive cells was found in layers II and III. Panel D: Several calbindin-containing neurons did not express Cre. Scale bars: 100 µm (A and C) and 20 µm (B and D).

Figure 6. Cre-expression in hipocampus of synapsin 1-Cre mice crossed with Ai9 reporter mice (see figure 3). Antibodies to neuronal markers NeuN (green; 1: 500; A-D) and parvalbumin (Parv, green; 1 µg/ml; E) were used to visualize neurons. Cre is present in some pyramidal cells (p) in CA1 (A and B), and is expressed a majority of pyramidal cells in CA3 (A and C). The tdTomato expression in the CA3 pyramidal cells (p) are hard to visualize due to the strong expression of tdTomato in the *stratum lucidum* (lu). However, a close look at panel C3 reveals a faint red color over the pyramidal cells. If they had been negative, then they would have been seen as black spots. This is clearly not the case for the majority of them. The strong expression in *stratum lucidum* is in agreement with the strong expression in the granule cells (gcl) in the dentate gyrus (DG: panels D and E). Also note that Cre is not expressed in parvalbumin-

positive interneurons in the dentate gyrus (E). Scale bars: 100 μm (A) and 20 μm (B-E).

Figure 7. Simplified scheme of ^{13}C-glucose metabolism leading to ^{13}C-labeling of amino acids and the increased uptake of glutamate into astrocytes and GABAergic neurons in the absence of EAAT2 in nerve terminals. A: Mice received uniformly ^{13}C-labeled glucose, which has a higher molecular weight (m+6) than unlabeled glucose. Uniformly ^{13}C-labeled glucose gives rise to uniformly ^{13}C-labeled pyruvate with molecular weight m+3. Pyruvate equilibrates with alanine, giving rise to alanine m+3, and it enters the TCA cycle as acetyl-CoA, in which the acetyl group has a molecular weight of m+2, leading to formation of m+2 species of glutamate, GABA, glutamine, and aspartate. Abbreviations: α-KG: α-ketoglutarate; OA: oxaloacetate. α-KG and OA are TCA cycle intermediates from which glutamate and aspartate are formed. B: Interpretation of data in Table 1: EAAT2 is silenced in glutamatergic nerve terminals, but uptake of ^{13}C-labeled glutamate into astrocytes and GABAergic neurons is maintained, leading to greater formation of ^{13}C-labeled glutamine and GABA. ^{13}C-Labeling is indicated by an asterisk.

Tables

	Alanine	Glutamate	Glutamine	GABA
WT (N=6)	32.7 ± 4.0	17.5 ± 1.8	11.6 ± 0.8	13.3 ± 0.9
nKO (N=4)	34.7 ± 5.3	19.5 ± 2.4	13.3 ± 0.4**	14.6 ± 0.6*

Table 1. ^{13}C-Labeling of amino acids in hippocampus after i.p. injection of [U-^{13}C]glucose.

Mice that were fasted overnight received [U-^{13}C]glucose, 7.5 μmol/g bodyweight i.p., and were killed after 15 minutes. Values are percent ^{13}C enrichment ± SD as calculated from the m+3 values for alanine and the m+2 values for glutamate, GABA, glutamine, aspartate. Alanine values reflect formation of [U-^{13}C]alanine from [U-^{13}C]pyruvate, which is derived from [U-^{13}C]glucose through glycolysis. M+2 values for the other amino acids reflect their labeling from [1,2-^{13}C]acetyl-CoA (which is formed from [U-^{13}C]pyruvate by pyruvate dehydrogenase), leading to formation of [4,5-^{13}C]glutamate and -glutamine, [1,2-^{13}C]GABA, and [3,4-^{13}C]- and [1,2-^{13}C]aspartate. Asterisks: difference from wild type animals; *: p=0.03; **: p= 0.004; two-tailed Student's *t*-test.

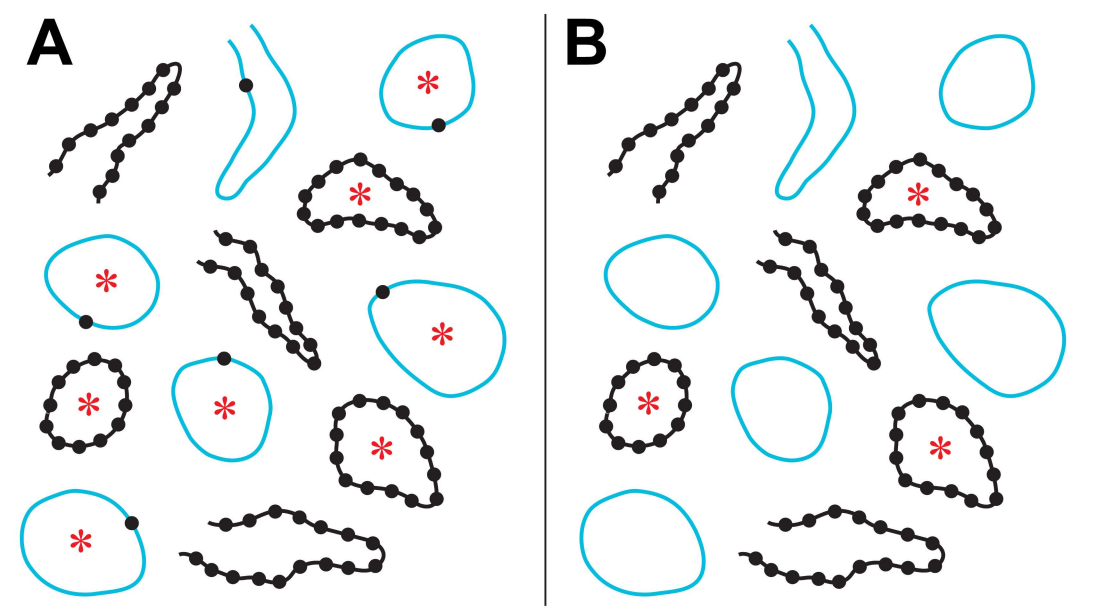

Figure 1

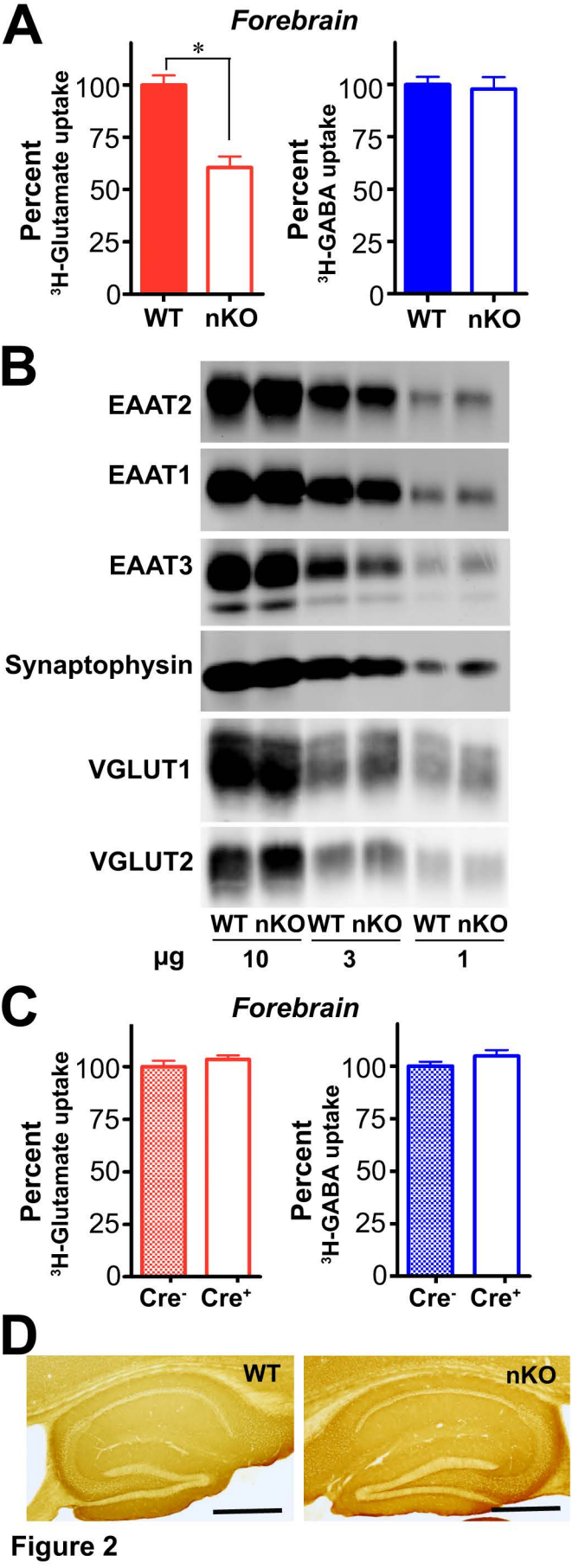
A
Forebrain
Percent
3H-Glutamate uptake
100
75
50
25
0
*
WT
nKO
Percent
3H-GABA uptake
100
75
50
25
0
WT
nKO
B
EAAT2
EAAT1
EAAT3
Synaptophysin
VGLUT1
VGLUT2
WT nKO WT nKO WT nKO
µg
10
3
1
C
Forebrain
Percent
3H-Glutamate uptake
100
75
50
25
0
Cre-
Cre+
Percent
3H-GABA uptake
100
75
50
25
0
Cre-
Cre+
D
WT
nKO

Figure 2

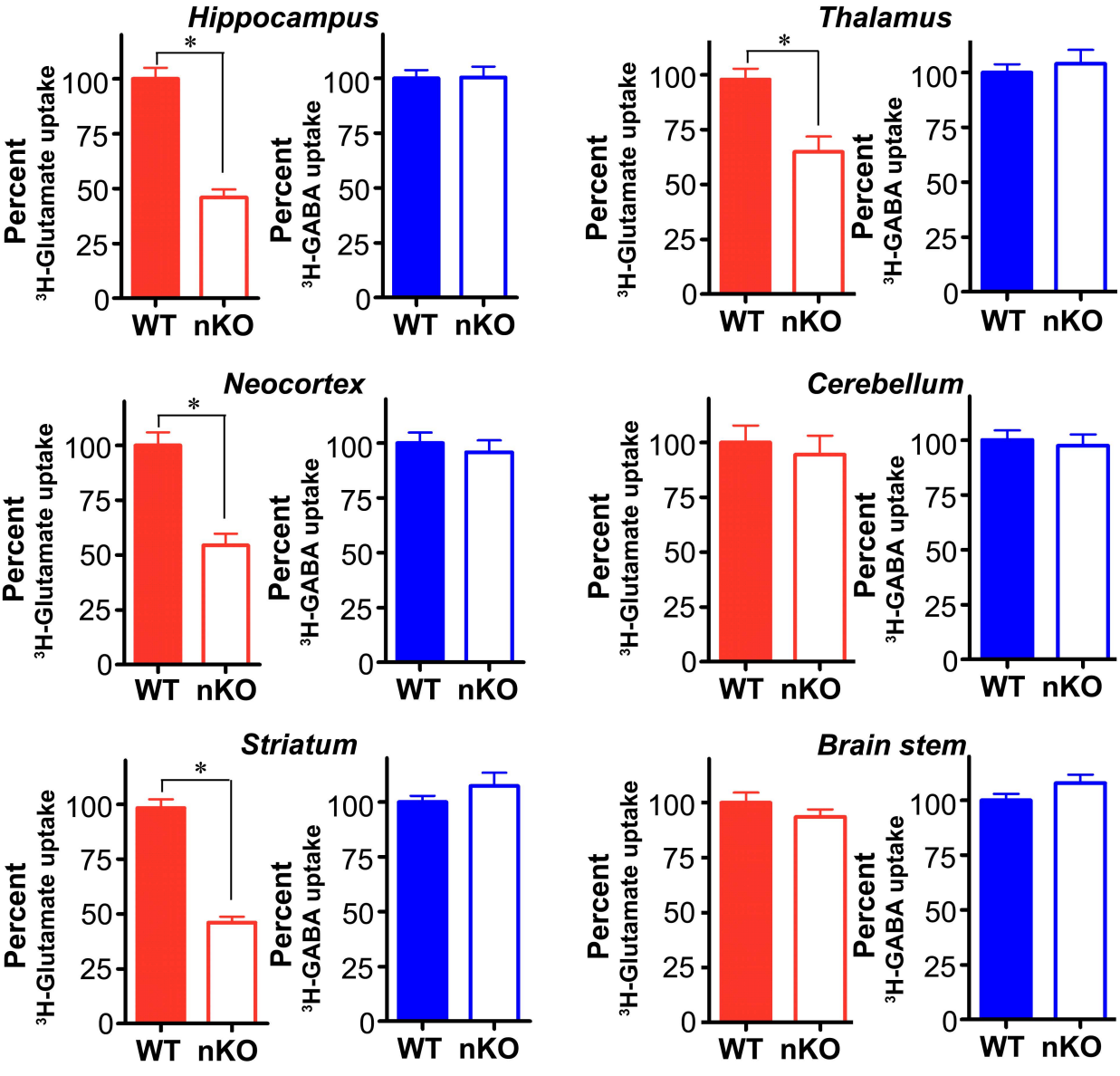
Hippocampus
Thalamus
Neocortex
Cerebellum
Striatum
Brain stem
Percent
^{3}H-Glutamate uptake
^{3}H-GABA uptake
100
75
50
25
0
*
WT
nKO

Figure 3

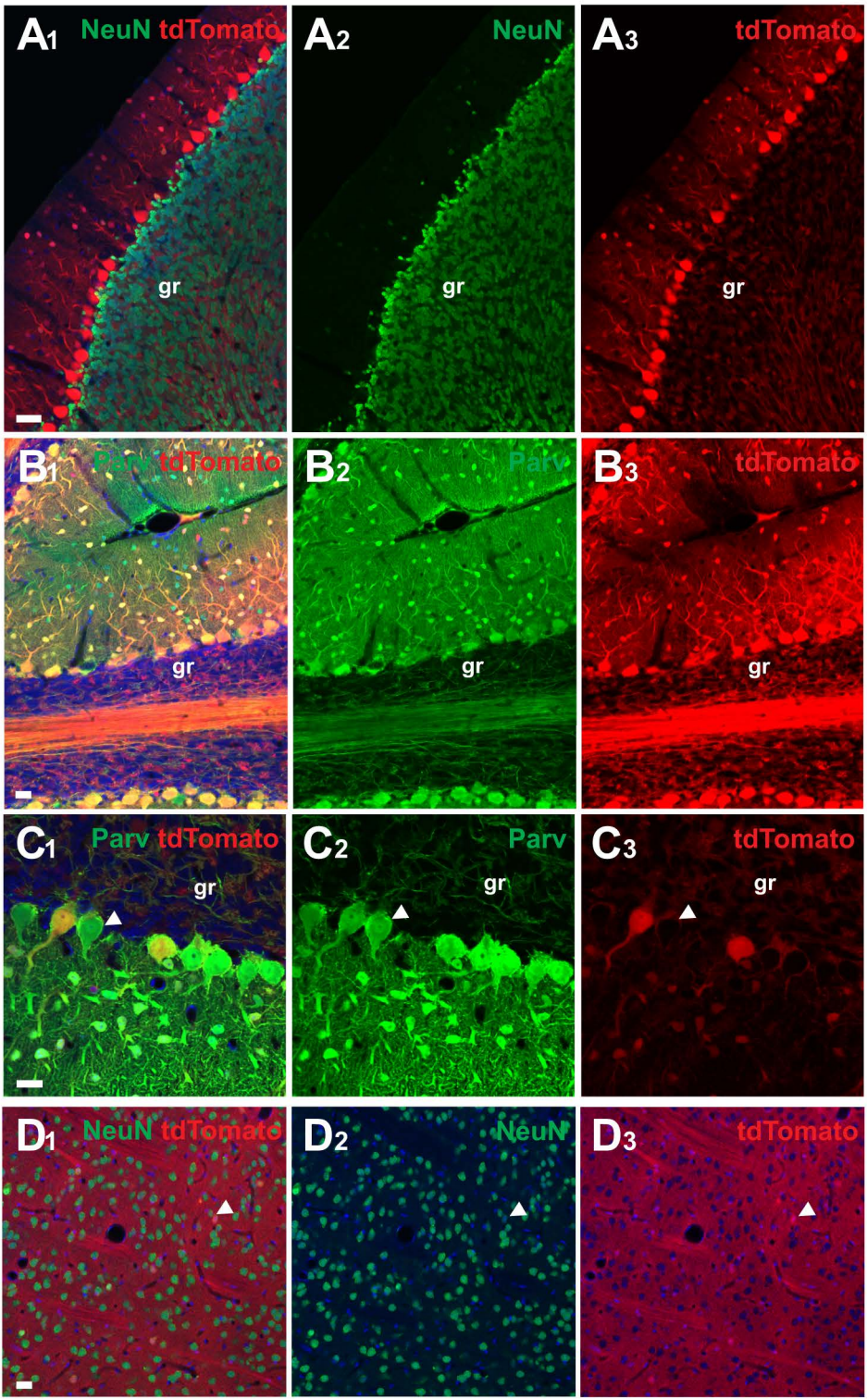
A1 NeuN tdTomato
gr
A2 NeuN
gr
A3 tdTomato
gr
B1 Parv tdTomato
gr
B2 Parv
gr
B3 tdTomato
gr
C1 Parv tdTomato
gr
C2 Parv
gr
C3 tdTomato
gr
D1 NeuN tdTomato
D2 NeuN
D3 tdTomato

Figure 4

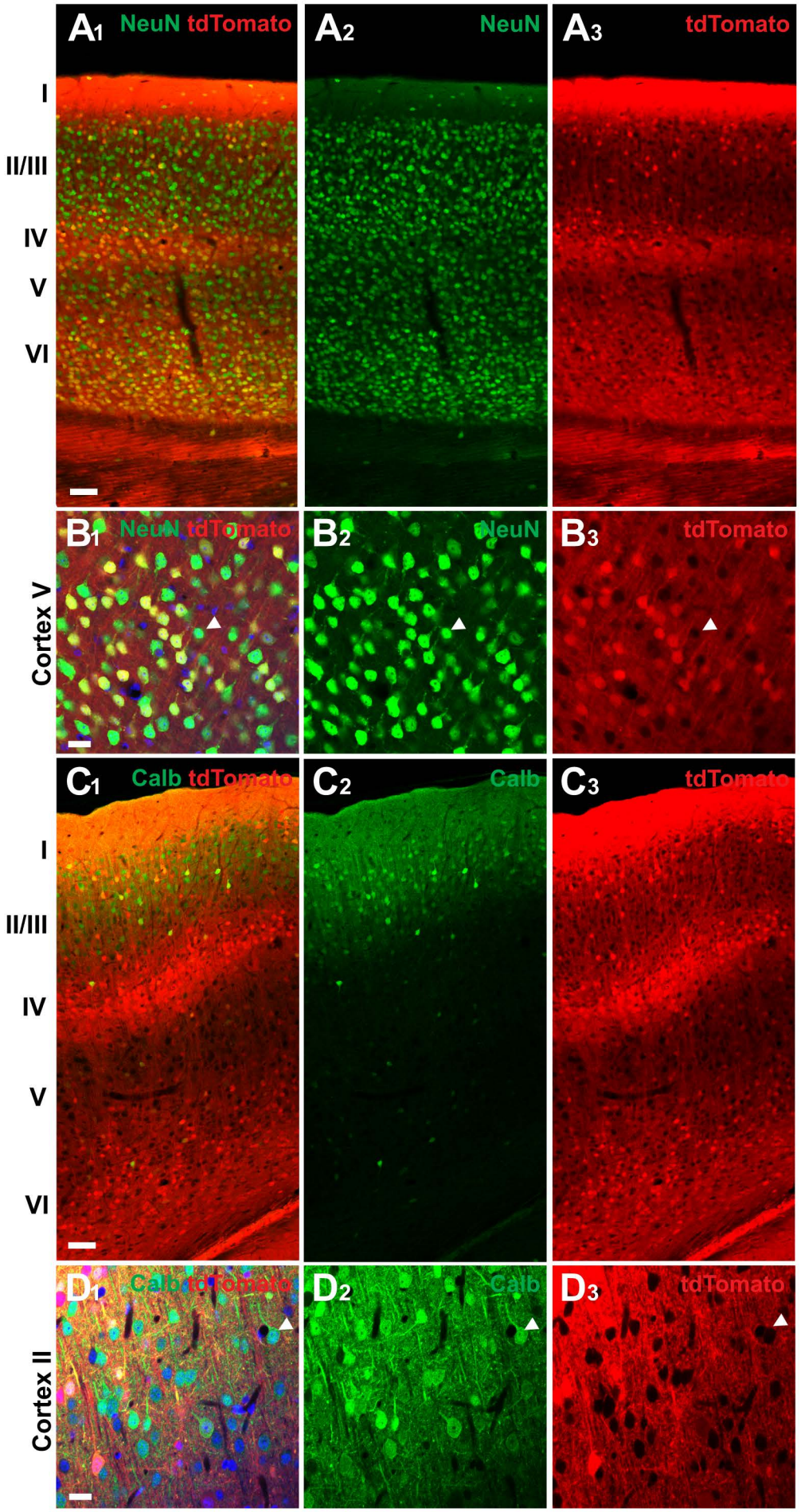
A1 NeuN tdTomato
A2 NeuN
A3 tdTomato
I
II/III
IV
V
VI
B1 NeuN tdTomato
B2 NeuN
B3 tdTomato
Cortex V
C1 Calb tdTomato
C2 Calb
C3 tdTomato
I
II/III
IV
V
VI
D1 Calb tdTomato
D2 Calb
D3 tdTomato
Cortex II

Figure 5

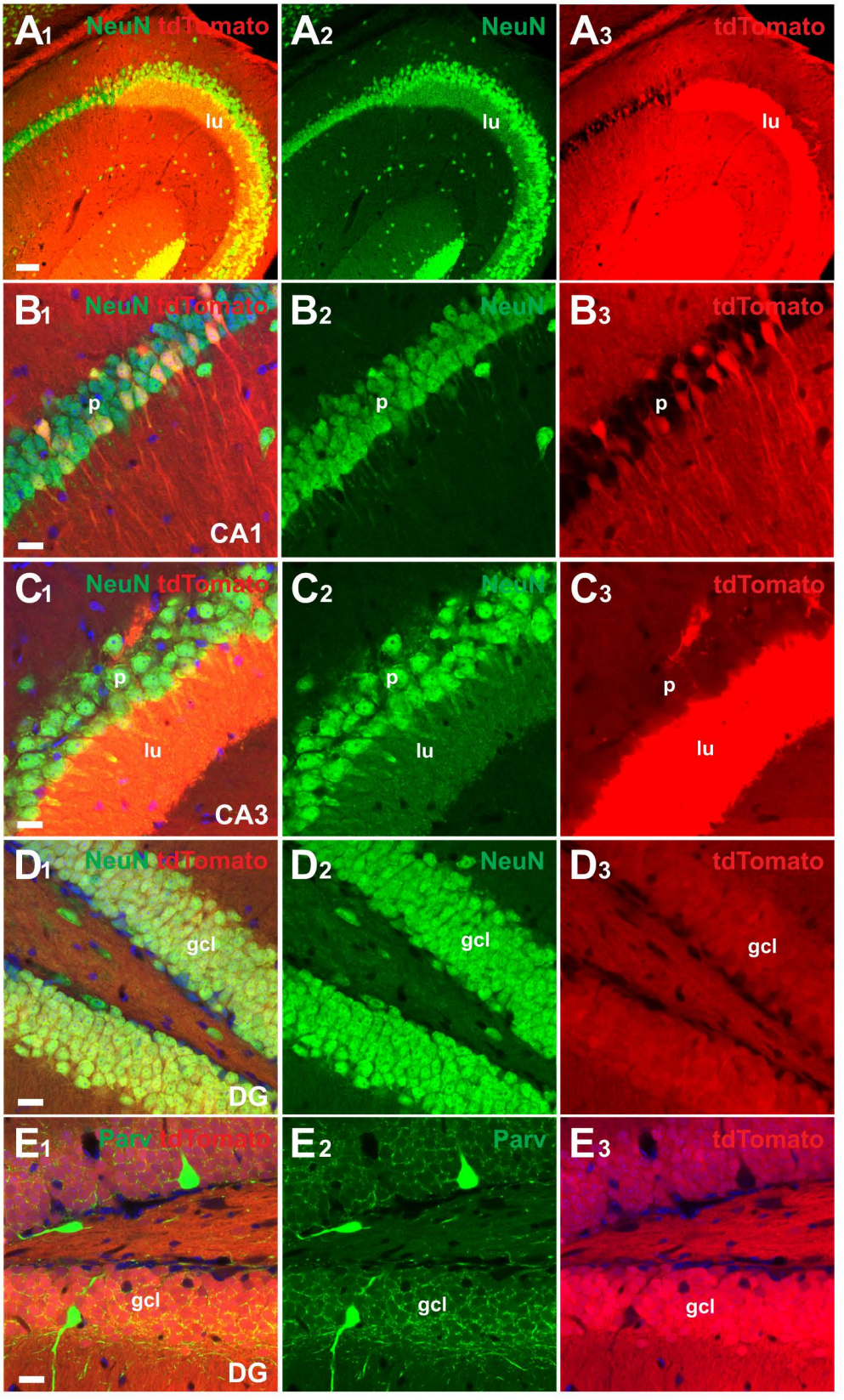
A1 NeuN tdTomato
lu
A2 NeuN
lu
A3 tdTomato
lu
B1 NeuN tdTomato
p
CA1
B2 NeuN
p
B3 tdTomato
p
C1 NeuN tdTomato
p
lu
CA3
C2 NeuN
p
lu
C3 tdTomato
p
lu
D1 NeuN tdTomato
gcl
DG
D2 NeuN
gcl
D3 tdTomato
gcl
E1 Parv tdTomato
gcl
DG
E2 Parv
gcl
E3 tdTomato
gcl

Figure 6

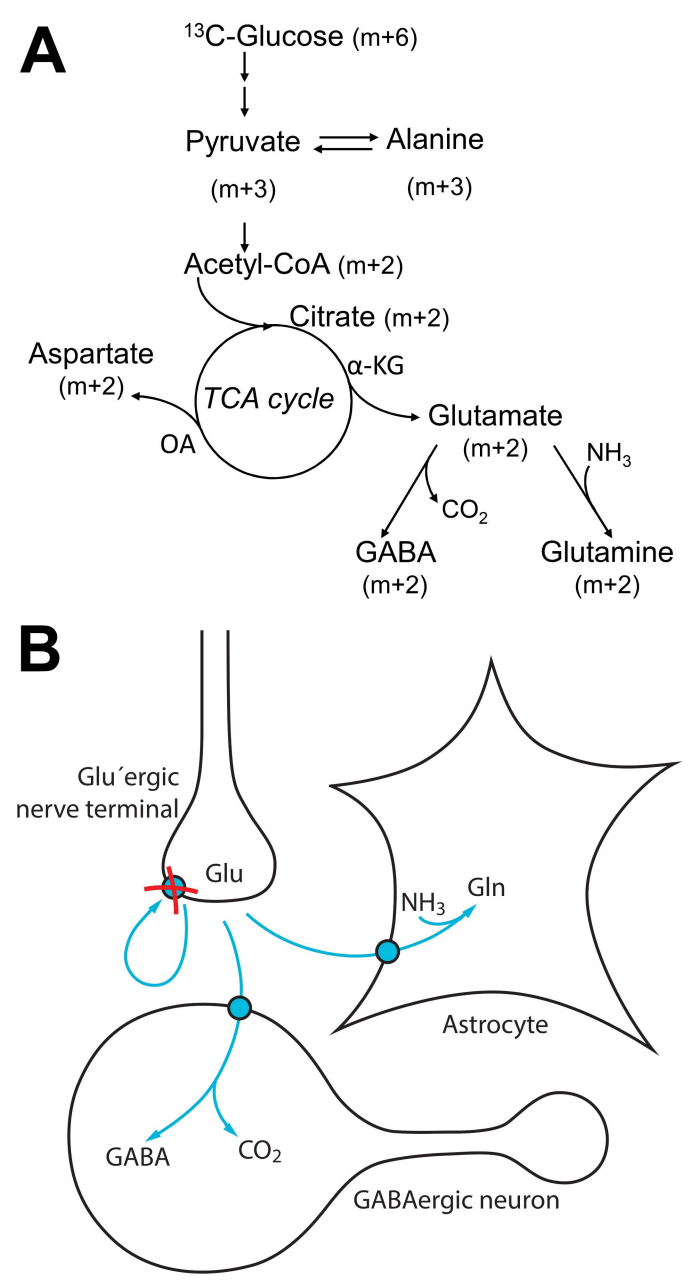
A
13C-Glucose (m+6)
Pyruvate
Alanine
(m+3)
(m+3)
Acetyl-CoA (m+2)
Citrate (m+2)
Aspartate
(m+2)
TCA cycle
α-KG
OA
Glutamate
(m+2)
NH3
CO2
GABA
(m+2)
Glutamine
(m+2)
B
Glu´ergic
nerve terminal
Glu
NH3
Gln
Astrocyte
GABA
CO2
GABAergic neuron

Figure 7